Bell States via Two-Particle Contact Interaction: Shannon Entropy as an Indicator of Entanglement Dynamics

Sandeep Mishra, Anjana Bagga, Anu Venugopalan*[1]

[1] *University School of Basic and Applied Sciences*
Guru Gobind Singh Indraprastha University, Sector 16 C, Dwarka, New Delhi-110078, India

(Dated: February 13, 2017)

We study the coherent dynamics of two interacting particles in a quantum double-well and show that the Shannon entropy can be a definitive signature of entanglement as an alternative to concurrence, a connection not reported previously. This physical model, involving tunneling and contact interaction, is akin to the Hubbard model which explains the physics of interacting particles in periodic potentials. We show that an interplay between tunneling and contact interaction produces Bell like eigenstates ensuring thereby that the concurrence and the Shannon entropy, two quantities with vastly different physical interpretations, develop the same time dependence. Our result, applied to three experimentally realized physical models works for both spatial and spin degrees of freedom and is significant as it provides a novel measure of entanglement applicable to many systems currently being explored for scalable quantum computation.

PACS numbers: 3.65.Ud, 3.67.Bg, 3.67.Mn, 89.70.Cf

arXiv:1702.00894v2 [quant-ph] 10 Feb 2017

The power and potential of quantum information is rooted in the singularly quantum phenomenon of *entanglement*. The concept describes a quantum state of a composite system of two (or more) particles which is non-separable and contains correlations that go beyond that predicted by classical theory [1, 2]. This uniquely quantum possibility has inspired many theoretical and experimental investigations involving the production and coherent manipulation of entangled states [3–8] with the aim of exploring new frontiers in computing power [9–11].

In this Letter, we propose a novel signature of entanglement through the Shannon entropy, making it an alternative experimental measure. For a two-particle system, Shannon (spatial) entropy captures the spread of the two particle wavefunction (localization) [12, 13] while the concurrence quantifies the degree of entanglement via correlations that reflect whether the two particle state is separable or not [14]. Thus, the two quantities seem to have vastly different physical interpretations. We examine two-particle entanglement dynamics via strong contact interaction and tunneling in a model akin to the Hubbard model recently explored in several experimental studies [7, 8, 15–18] and apply our result to three experimentally realized physical models incorporating spatial and spin degrees of freedom. We show that a measurement of Shannon entropy reflects entanglement dynamics.

To demonstrate our result, we consider a system of two distinguishable particles in a one dimensional infinite square well potential with a δ barrier at its center. Each particle can tunnel between the two wells. For an opaque barrier [19, 20] this system is equivalent to two qubits [21] where $|L\rangle$ and $|R\rangle$ represent two orthogonal single qubit states, corresponding to left and right localization in the double well. The tunneling eigenstates, $|\phi\rangle$ and $|\tilde{\phi}\rangle$ are linear superpositions of $|L\rangle$ and $|R\rangle$ (see Fig. 1(a)). The inclusion of contact interaction between the two particles provides a mechanism for entanglement. The system can be described by the Hamiltonian:

$$H = \sum_{i=1,2} \epsilon_0 I^{(i)} + \Delta \sum_{i=1,2} \sigma_x^{(i)} + U\sigma_z^{(1)} \otimes \sigma_z^{(2)}, \qquad (1)$$

where ϵ_0 is the lowest single particle energy when confined in either well, Δ is the tunneling strength and U is the contact interaction strength . The ratio U/Δ determines the energy eigenvalue spectrum of the Hamiltonian (1) and the nature of its eigenfunctions (see Fig. 2). For $U/\Delta \gtrsim 4$, i.e., when the contact interaction dominates the tunneling, the four eigenstates of (1), $\{|ES_i\rangle\}$, become nearly Bell states [9] in the two particle positional basis of $|LL\rangle, |LR\rangle, |RL\rangle$ and $|RR\rangle$ (Fig.1(c)):

$$\begin{aligned} |ES_1\rangle, |ES_2\rangle &\approx \Psi^{\pm} \approx \frac{1}{\sqrt{2}}(|LR\rangle \pm |RL\rangle), \qquad (2) \\ |ES_3\rangle, |ES_4\rangle &\approx \Phi^{\mp} \approx \frac{1}{\sqrt{2}}(|LL\rangle \mp |RR\rangle). \end{aligned}$$

The distinctive eigenvalue spectrum of Fig. 2(c) is crucial to the dynamics which correlates the time dependence of the Shannon entropy and concurrence.

In Fig. 2(a), $U = 0$ (contact interaction is absent) and hence there is no entanglement and the two particles independently tunnel between wells. The eigenstates here are each equally weighted linear combinations of $|LL\rangle, |LR\rangle, |RL\rangle$ and $|RR\rangle$, with $|ES_2\rangle$ and $|ES_3\rangle$ degenerate and separated from $|ES_1\rangle$ and $|ES_4\rangle$ by a gap proportional to Δ. When a repulsive contact interaction is introduced between the two particles, the degeneracy of Fig. 2(a) is lifted and the eigenvalue spectrum modifies, shifting the states $|LL\rangle$ and $|RR\rangle$ higher compared to the states $|LR\rangle$ and $|RL\rangle$ (see Fig. 2(b)). The repulsive interaction makes states $|LL\rangle$ and $|RR\rangle$ (both particles in the

same well), energetically more expensive than $|LR\rangle$ and $|RL\rangle$ (each particle in a separate well). Consequently, the two lower energy eigenstates have a higher probability amplitude corresponding to $|LR\rangle$ and $|RL\rangle$ and the higher energy eigenstates have a higher probability amplitude corresponding to $|LL\rangle$ and $|RR\rangle$ as shown in Fig. 2 where $p > q$ and p and q depend on the parameters U and Δ. When the contact interaction is much stronger than the tunneling strength ($U/\Delta \gtrsim 4$, see Fig. 2(c)) the eigenstates become nearly Bell states (2), with the Bell states $|\Phi^{\pm}\rangle$ (in $|LL\rangle$ and $|RR\rangle$) widely separated from $|\Psi^{\pm}\rangle$ (in $|LR\rangle$ and $|RL\rangle$) by an amount proportional to $2U$. Additionally, $E_4 - E_3 \approx E_2 - E_1 \ll U$ as illustrated in Fig. 2(c). The ratio $U/\Delta \gtrsim 4$ is close to the parameter regimes explored in several recent experiments [8, 15, 22–24].

We now show how the unique eigenvalue spectrum of Fig. 2(c) is instrumental in making the Shannon (spatial) entropy mimic entanglement dynamics. Consider a general two-particle initial state

$$\psi(x_1, x_2, 0) = \sum_{i=1,4} c_i |ES_i\rangle, \tag{3}$$

where x_1 and x_2 are the position coordinates of each particle and $\{c_i\}s$ are the overlap amplitudes of the initial state with the eigenstates $\{|ES_i\rangle\}$. The time evolution (3), driven by the eigenvalue spectrum of (1) is:

$$\psi(x_1, x_2, t) = \sum_{i=1,4} c_i |ES_i\rangle e^{-iE_i t/\hbar}, \tag{4}$$

where $\{E_i\}$s are energy eigenvalues and t is the time. Eq. (4), expressed in the positional basis of $|LL\rangle, |LR\rangle, |RL\rangle$ and $|RR\rangle$ is:

$$\begin{aligned} \psi(x_1, x_2, t) &= \alpha_{LL}|LL\rangle + \alpha_{LR}|LR\rangle \\ &\quad + \alpha_{RL}|RL\rangle + \alpha_{RR}|RR\rangle, \end{aligned} \tag{5}$$

where $\alpha_{LL} = \sum_{i=1,4} c_i \langle LL|ES_i\rangle e^{-iE_i t/\hbar}$ represents the overlap amplitude of the state $|LL\rangle$ with the eigenstates $\{|ES_i\rangle\}$ and α_{LR}, α_{RL} and α_{RR} can each be defined in a similar manner. When $U/\Delta \gtrsim 4$, the eigenstates $\{|ES_i\rangle\}$ become nearly Bell states (Fig. 2(c)) with α_{LL} and α_{RR} such that $c_1 \approx 0$, $c_2 \approx 0$, $c_3 \neq 0$, $c_4 \neq 0$, while for α_{LR} and α_{RL}, $c_1 \neq 0$, $c_2 \neq 0$, $c_3 \approx 0$, $c_4 \approx 0$. From the overlap amplitudes α_{LR}, α_{RL} , α_{LL}, and α_{RR} the corresponding probabilities, P_{LR}, P_{RL}, P_{LL} and P_{RR} for the state (5) are :

$$\begin{aligned} P_{LR}, P_{RL} &= \frac{c_1^2}{2} + \frac{c_2^2}{2} \pm c_1 c_2 \cos\left[\frac{(E_2 - E_1)t}{\hbar}\right], \\ P_{LL}, P_{RR} &= \frac{c_3^2}{2} + \frac{c_4^2}{2} \pm c_3 c_4 \cos\left[\frac{(E_4 - E_3)t}{\hbar}\right]. \end{aligned} \tag{6}$$

It is clear from (6) that the probabilities vary sinusoidal with time, governed only by the low frequencies shown in Fig. 2(c). P_{LR}, P_{RL}, P_{LL} and P_{RR} capture probabilities for the presence (spatial localization) of the two particles in the right and left wells as a function of time and determine the two-particle spatial (Shannon) entropy:

$$\begin{aligned} S_H(t) &= -\{P_{LL}\log_2 P_{LL} + P_{LR}\log_2 P_{LR} \\ &\quad + P_{RL}\log_2 P_{RL} + P_{RR}\log_2 P_{RR}\} \end{aligned} \tag{7}$$

$$\approx A\left\{\frac{c_3^2}{2}\frac{c_4^2}{2}\cos\left[\frac{2(E_4 - E_3)t}{\hbar}\right] + \frac{c_1^2}{2}\frac{c_2^2}{2}\cos\left[\frac{2(E_2 - E_1)t}{\hbar}\right]\right\} + C_0,$$

where A and C_0 are constants. Spatial (Shannon) entropy as understood above measures localization in the state space (defined here by $|L\rangle$ and $|R\rangle$ for each particle) of the two-particle system and is zero if the two particles are both localized in either well, i.e., if only one of the probabilities in (7) is non zero. Also, S_H is maximum when it is equally probable for each particle to be in both wells. We emphasize that the time dependence of the spatial (Shannon) entropy as seen in (7) is governed only by low frequencies shown in Fig. 2(c).

Concurrence [14], a standard measure for quantifying entanglement in pure bipartite systems can be written for the two-particle state (5) as:

$$C(\psi) = 2|\alpha_{LL}\alpha_{RR} - \alpha_{LR}\alpha_{RL}|, \tag{8}$$

with $C > 0$ corresponding to entangled states and $C = 1$ corresponding to maximally entangled states (Bell states). The modulus square of the concurrence is

$$\begin{aligned} |C|^2 = &\left\{\frac{c_3^2}{2}\frac{c_4^2}{2}\cos\left[\frac{2(E_4 - E_3)t}{\hbar}\right] + \frac{c_2^2}{2}\frac{c_1^2}{2}\cos\left[\frac{2(E_2 - E_1)t}{\hbar}\right]\right\}_{\mathbf{L}} \\ &+\left\{\frac{c_2^2}{2}\frac{c_4^2}{2}\cos\left[\frac{2(E_4 - E_2)t}{\hbar}\right] + \frac{c_3^2}{2}\frac{c_2^2}{2}\cos\left[\frac{2(E_3 - E_2)t}{\hbar}\right]\right. \\ &\left.+\frac{c_1^2}{2}\frac{c_4^2}{2}\cos\left[\frac{2(E_4 - E_1)t}{\hbar}\right] + \frac{c_3^2}{2}\frac{c_1^2}{2}\cos\left[\frac{2(E_3 - E_1)t}{\hbar}\right]\right\}_{\mathbf{H}} + C_1, \end{aligned} \tag{9}$$

where C_1 is a constant. Eq. (9) is a sum of terms containing all transition frequencies seen in the energy spectrum emerging when $U/\Delta \gtrsim 4$ (Fig. 2(c)). This allows us to put the terms in $|C|^2$ into two categories: low (**L**) and high (**H**) frequency terms. Further, it is possible to write the high frequency part (**H**) as sums of cosine terms whose arguments differ by small amount $\Delta\omega(\approx (E_4 - E_3)/\hbar \approx (E_2 - E_1)/\hbar)$, as is usually seen in the beats phenomenon. This way, we can show that these terms combine such that $|C|^2$ has a form that resembles a beat-like phenomenon:

$$\begin{aligned} |C|^2 &= B\left\{\frac{c_3^2}{2}\frac{c_4^2}{2}\cos\left[\frac{2(E_4 - E_3)t}{\hbar}\right]\right. \\ &\quad \left.+\frac{c_2^2}{2}\frac{c_1^2}{2}\cos\left[\frac{2(E_2 - E_1)t}{\hbar}\right] + \alpha\right\}_{\mathbf{I}} \\ &\quad \times\left\{\beta\cos\left[\frac{2(E_3 - E_1)t}{\hbar} + \theta\right] + 1\right\}_{\mathbf{II}} \end{aligned} \tag{10}$$

where B, α and β are constants and $\beta = \left\{(c_3^2+c_4^2)(c_1^2+c_2^2) - |c_4^2-c_3^2||c_2^2-c_1^2|\right\} / \left\{2\left(c_3^2c_4^2+c_1^2c_2^2\right)\right\}$ and θ is a function of $\{c_i\}s$ and time. The expression for $|C|^2$, (10), clearly contains a high frequency term (**II**) modulated by a slowly varying envelope term (**I**) (see Figs. 3 and 4). Eqs. (7) and (10) capture the time dependence of the Shannon entropy and the square of the concurrence, respectively, for (1) when $U/\Delta \gtrsim 4$. The envelope in (10) captures amplitude variations of the value of the square of the concurrence. More significantly, (7) and (10) show that the time dependence of the envelope of the square of the concurrence (and hence of the concurrence) is similar to that of the spatial (Shannon) entropy, implying thereby that an experimental measurement of spatial entropy can clearly be an alternative indicator of entanglement. Next, we apply this result to three different experimentally realized physical models.

First, we look at a system of two neutral cold atoms trapped in an optically created double well, explored in many recent experiments [7, 8, 15–17]. Advanced techniques allow the control of interparticle interactions between the atoms with high precision [8, 15, 16]. Recently, Murmann et al. have trapped two ultracold Lithium atoms (each in two different hyper-fine states, $|\uparrow\rangle = |F=\frac{1}{2}m=+\frac{1}{2}\rangle$ and $|\downarrow\rangle = |F=\frac{1}{2}m=-\frac{1}{2}\rangle$) into the motional ground state of an optical dipole trap mimicing a double well and introduced a repulsive interparticle interaction between them [8]. They independently control this interparticle interaction strength as well as the tunneling rate between the two wells [8].

To compare the dynamics of the spatial entropy and the envelope of square of the concurrence, the values of the parameters Δ (tunneling strength) and U(contact interaction strength) used in the experiment of Murmann et al are chosen for the Hamiltonian (1)(see Table I). Fig. 3 shows plots of the spatial (Shannon) entropy and square of the concurrence for four different initial states. In Fig. 3(a) the initial state is $|LL\rangle$ for which the coefficients, $\{c_i\}s$ are such that $c_1=0$, $c_2=0$ and $c_3=c_4=1/\sqrt{2}$. Thus, the time evolution of $|LL\rangle$ is governed only by the eigenstates $|ES_3\rangle$ and $|ES_4\rangle$ involving only the low frequency $(E_4-E_3)/\hbar$ (see Fig. 2(c)). As a result both spatial entropy and concurrence have the same sinusoidal time dependence, governed by $2(E_4-E_3)/\hbar$. This is also evident when the values of the coefficients, $\{c_i\}s$, are put in Eqs. (7) and (10). The absence of high frequency oscillations in the square of the concurrence for the initial state $|LL\rangle$ can be appreciated by noting that in Eq.(8), α_{LR} and α_{RL} are zero for $|LL\rangle$ and hence there is no interference between the two terms.

Fig. 3(b) shows spatial (Shannon) entropy and square of the concurrence for an initial state $\frac{1}{\sqrt{2}}\{|LL\rangle + |LR\rangle\}$ with $c_1=c_2=c_3=c_4=1/2$. Here, the square of the concurrence shows fast oscillations modulated by a slow envelope whose time dependence is similar to that of the spatial entropy. The time dependence of the spatial entropy and the envelope of the square of the concurrence, as seen from (7) and (10), are determined by a summation of two cosine terms, where the argument of cosine terms are small and nearly equal (i.e., $E_4-E_3 \approx E_2-E_1$ (see Fig. 2(c)). The fast oscillations in the square of the concurrence is due to the high frequency term in Eq.(10) which arises due to the interference between two terms in Eq.(8). Fig. 3(c) shows the plots for the initial state $\frac{1}{\sqrt{3}}\{|LL\rangle + |RR\rangle + |LR\rangle\}$ with $c_1=c_2=1/\sqrt{6}, c_3=0, c_4=\sqrt{2/3}$ where it can again be seen that spatial entropy and envelope of square of the concurrence have similar time dependence for the same reasons as Fig. 3(b). Fig. 3(d) shows the plots for the initial state $\frac{1}{2}\{|LL\rangle + |RR\rangle + |LR\rangle + |RL\rangle\}$ with $c_1=1/\sqrt{2}, c_2=0, c_3=0, c_4=1/\sqrt{2}$. Here both spatial entropy and the envelope of the square of the concurrence are constant with time which can be verified by putting the values of the coefficients, $\{c_i\}s$ in (7) and (10). Alternately, one can appreciate this by observing that the time evolution of the initial state here is $1/2(|LR\rangle + |RL\rangle)e^{iE_1t/\hbar} + 1/2(|LL\rangle + |RR\rangle)e^{iE_4t/\hbar}$, where all the probabilities $P_{LL}, P_{RR}, P_{LR}, P_{RL}$ become independent of time, making the spatial entropy and the envelope of the concurrence independent of time. The high frequency oscillations continue to be present in the concurrence here as the two interfering terms in (8) are non zero. Thus, we conclude that for any initial state the time dependence of the spatial (Shannon) entropy and the envelope of concurrence is similar and they attain their maxima and minima at the same times.

Next, we apply our result to a physical system simulating quantum magnets. Laser cooling techniques that trap cold atoms into optical lattices allow for the study of not only motional states of atoms but also internal spin degrees [24, 25]. Recently, Friedenauer et al have explored quantum magnetization for two confined spin-1/2 particles where entanglement dynamics arises from an interplay between tunneling and spin-spin interaction [24]. In their system, each spin is represented by two hyperfine ground levels of trapped $^{25}Mg^+$ ions in the $^2S_{1/2}$ state. The spin states $|\downarrow\rangle = |F=3; m_f=3\rangle$ and $|\uparrow\rangle = |F=2; m_f=2\rangle$ are analogous to $|L\rangle$ and $|R\rangle$ in our previous example of cold atoms, and $\frac{1}{\sqrt{2}}\{|\uparrow\rangle \pm |\downarrow\rangle\}$ are analogous to the tunneling eigenstates in position, $\frac{1}{\sqrt{2}}\{|L\rangle \pm |R\rangle\}$, resulting from the interaction of each spin with a uniform magnetic field B_x [24]. B_x is simulated by coherently coupling the hyperfine levels via laser and radio frequency radiation and is analogous to the tunneling strength, Δ. The spin-spin interaction, U, is experimentally realized by interacting the $^{25}Mg^+$ ions with laser beams which induce a state dependent optical dipole force via the ac stark shift [24]. It may be noted that the Shannon entropy (7) here derives from $P_{\uparrow\uparrow}$ $P_{\uparrow\downarrow}$, $P_{\downarrow\uparrow}$, $P_{\downarrow\downarrow}$, corresponding to spin. The actual ex-

perimental parameters B_x and U (see Table I) are used to compare concurrence and Shannon (spin) entropy and we find that they show a similar time dependence. This holds true for any initial state and is illustrated in Fig. 4(b) for the initial state $\frac{1}{\sqrt{2}}\{|\uparrow\uparrow\rangle + |\downarrow\downarrow\rangle\}$.

Finally, we demonstrate our results for two electrons confined in quantum molecules, which are double quantum dot (DQD) structures where an electron can tunnel from one quantum dot to another [22, 26–28]. Such systems are promising candidates for quantum hardware in quantum computing. Shinkai et al [22] have recently investigated the dynamics of two electrons confined in separate quantum molecules mimicking the model described in this work. The two electrons can each tunnel between the two wells of a DQD and can also interact electrostatically with each other [22]. Both the tunneling strength, Δ, and the electrostatic interaction strength, U, can be experimentally controlled. Oliveira and Sanz have recently analyzed the two particle entanglement dynamics for this experiment [23]. As before, an interplay of tunneling and interaction leads to the formation of Bell states in the basis $|LL\rangle$, $|LR\rangle$, $|RL\rangle$ and $|RR\rangle$. We use the parameter values for Δ and U from the experiment of Shinkai et al (see Table I) to show that the spatial entropy and the envelope of the concurrence have the same time dependence and attain their maxima and minima at the same times (see Fig. 4(c)).

To conclude, our study of the coherent dynamics of two particles in a quantum double-well shows that the concurrence, a measure of entanglement, can be written as a beat like phenomenon with fast oscillations modulated by a slowly varying envelope when the contact interaction dominates the tunneling strength. More significantly, we show that the Shannon entropy, conventionally reflecting the spread in probabilities of the two particle state, has the same time dependence as that of the envelope of the concurrence, making it a definitive measurable signature of entanglement. This connection between the concurrence and the Shannon entropy, two quantities with vastly different physical interpretations, has not been reported previously. Our model is akin to the Hubbard model that explains the physics of interacting particles in periodic potentials and ultracold atoms in optical traps simulating qubits and quantum gates. We illustrate our result in three experimentally realized physical models having both spatial and spin degrees of freedom. Our result gives a novel, experimentally accessible measure of entanglement applicable in physical systems that can be explored for quantum information and scalable quantum computation.

*Corresponding author
anu.venugopalan@gmail.com

[1] E. Schrödinger, Proc. Cambridge Philos. Soc. **31**, 555 (1935).
[2] A. Einstein, B. Podolsky, and N. Rosen, Phy. Rev. **47**, 77 (1935).
[3] C. Monroe, D. M. Meekhof, B. E. King and D. Wineland, Science **272**, 1131 (1996).
[4] R. Blatt and D. Wineland, Nature(London) **453**, 1008 (2008).
[5] D. Jaksch, H.J. Briegel, J. I. Cirac, C. W. Gardiner and P. Zoller, Phys. Rev. Lett. **82**, 1975 (1999).
[6] I. Bloch, Nature(London) **453**, 1016 (2008).
[7] J. Mompart, K. Eckert, W. Ertmer, G. Birkl and M. Lewenstein, Phys. Rev. Lett. **90**, 147901 (2003).
[8] S. Murmann, A. Bergschneider, V. M. Klinkhamer, G. Zürn, T. Lompe and S. Jochim, Phys. Rev. Lett. **114**, 080402 (2015).
[9] M. A. Nielsen, I. L. Chuang, *Quantum Computation and Quantum Information* (Cambridge University Press, New Delhi, 2008).
[10] D. Bouwmeester, J. W. Pan, K. Mattle, M. Eibl, H. Weinfurter and A. Zeilinger, Nature(London) **390**, 575 (1997).
[11] A. K. Ekert, Phys. Rev. Lett. **67**, 661 (1991).
[12] E. Romera and F. de los Santos, Phys. Rev. Lett. **99**, 263601 (2007).
[13] I. Bialynicki-Birula and J. Mycielski, Commun. Math. Phys. **44**, 129 (1975).
[14] S. Hill and W. K. Wootters, Phys. Rev. Lett. **78**, 5022 (1997); W. K. Wootters, *ibid.* **80**, 2245 (1998).
[15] S. Fölling, S. Trotzky, P. Cheinet, M. Feld, R. Saers, A. Widera, T. Muller and I. Bloch, Nature(London) **448**, 1029 (2007).
[16] G. Zürn, F. Serwane, T. Lompe, A. N. Wenz, M. G. Ries, J. E. Bohn and S. Jochim, Phys. Rev. Lett. **108**, 075303 (2012).
[17] F. W. Strauch, M. Edwards, E. Tiesinga, C. Williams and C. W. Clark, Phys. Rev. A **77**, 050304 (2008).
[18] F. H. Essler, H. Frahm, F. Ghmann, A. Klmper and V. E. Korepin, *The one-dimensional Hubbard model* (Cambridge University Press, Cambridge, 2005).
[19] P. Senn, Am. J. Phys. **60**, 228 (1992).
[20] G. A. Vugalter, A. K. Das and V. A. Sorokin, Phys. Rev. A **66**, 012104 (2002).
[21] C. J. Foot and M. D. Shotter, Am. J. Phys. **79**, 762 (2011).
[22] G. Shinkai, T. Hayashi, T. Ota and T. Fujisawa, Phys. Rev. Lett. **103**, 056802 (2009).
[23] P. A. Oliveira and L. Sanz, Ann. Phys.(NY) **356**, 244 (2015).
[24] A. Friedenauer, H. Schmitz, J. T. Glueckert, D. Porras, and T. Schaetz, Nature Physics **4**, 757 (2008).
[25] J. Simon, W. S. Bakr, R. Ma, M. E. Tai, P. M. Preiss and M. Greiner, Nature(London) **472**, 307 (2011).
[26] J. R. Petta, A. C. Johnson, J. M. Taylor, E. A. Laird, A. Yacoby, M. D. Lukin, C. M. Marcus, M. P. Hanson, and A. C. Gossard, Science **309**, 2180 (2005)
[27] T. Hayashi, T. Fujisawa, H. D. Cheong, Y. H. Jeong and Y. Hirayama, Phys. Rev. Lett. **91**, 226804 (2003).
[28] G. Shinkai, T. Hayashi, Y. Hirayama and T. Fujisawa, Appl. Phys. Lett. **90**, 103116 (2007).

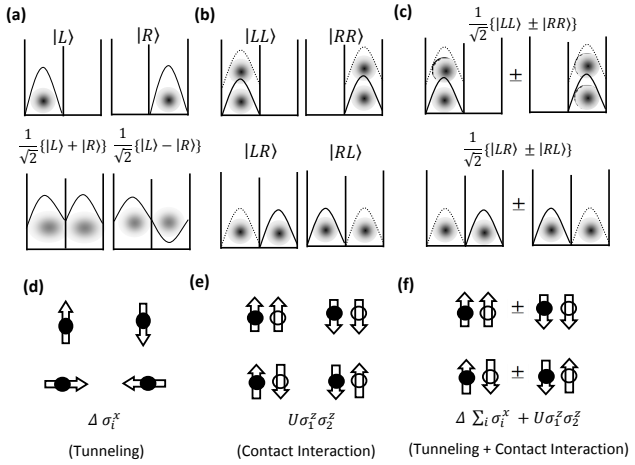

FIG. 1: (a) Infinite square well with δ barrier in the center; single particle states $|L\rangle$ and $|R\rangle$; tunneling eigenstates states $\frac{1}{\sqrt{2}}\{|L\rangle \pm |R\rangle\}$. (b) Two particle eigenstates $|LL\rangle, |LR\rangle, |RL\rangle$ and $|RR\rangle$ in the presence of contact interaction. (c) Eigenstates of $\Delta \sum_{i=1,2} \sigma_x^{(i)} + U\sigma_z^{(1)} \otimes \sigma_z^{(2)}$ for $U/\Delta \gtrsim 4$. (d), (e), (f) corresponding states for spin.

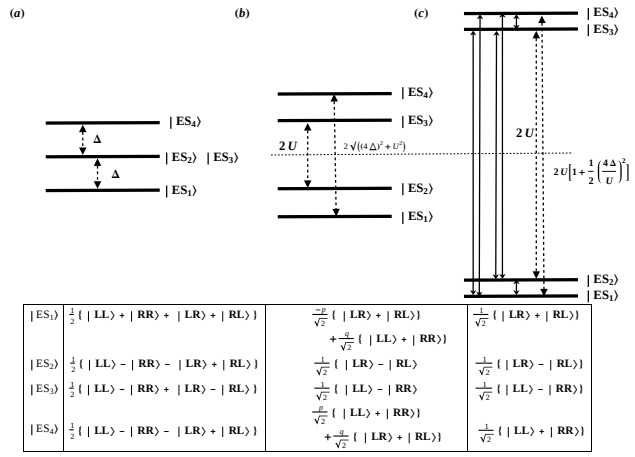

FIG. 2: Energy eigenvalues and eigenstates for (a) $U = 0$, eigenstates equally weighted superpositions of $|LL\rangle, |LR\rangle, |RL\rangle$ and $|RR\rangle$ (b) $U \approx \Delta$, $|LL\rangle$ and $|RR\rangle$ raised in energy compared to $|LR\rangle$ and $|RL\rangle$ due to contact interaction making the probability amplitudes for $|LR\rangle$ and $|RL\rangle$ higher than $|LL\rangle$ and $|RR\rangle$ in $|ES_1\rangle$, $|ES_2\rangle$ and vice versa for $|ES_3\rangle$, $|ES_4\rangle$ $(p > q)$, (c) $U/\Delta \gtrsim 4$, eigenstates become nearly Bell states and $|ES_1\rangle$, $|ES_2\rangle$ are widely separated from $|ES_3\rangle$, $|ES_4\rangle$ by an amount proportional to $2U$.

TABLE I: Details and parameter values for three physical models

System	Particles	Bell state basis	U(eV)	Δ (eV)	U/Δ	Time Scale $(\frac{h}{2(E_4-E_3)})$(s)
Optical trap	Neutral atoms (^6Li)	Positional	2.7×10^{-12}	2.66×10^{-13}	10	124 ms
Quantum magnet	Ion($^{25}Mg^+$)	Spin	91.1×10^{-12}	17.5×10^{-12}	5.2	0.31 ms
Semiconductor DQD	Charged particle (e^-)	Positional	25×10^{-6}	6.25×10^{-6}	4	10.1 ns

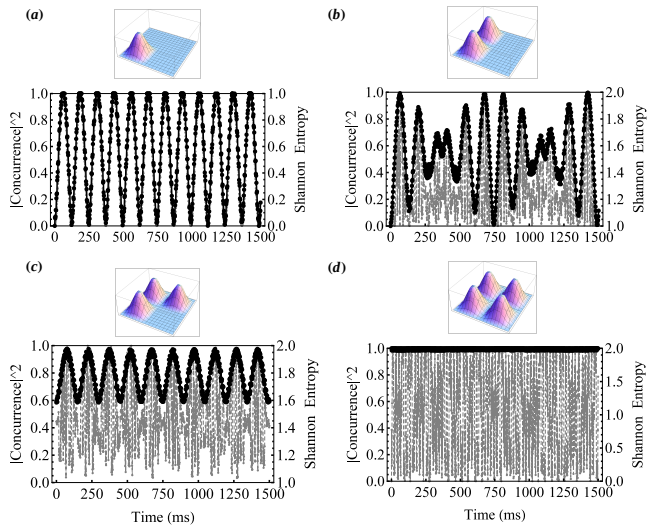

FIG. 3: Time evolution of Shannon (spatial) entropy (black) and $|\text{concurrence}|^2$ (gray) for four initial states (a) $|LL\rangle$ (b) $\frac{1}{\sqrt{2}}\{|LL\rangle + |LR\rangle\}$ (c) $\frac{1}{\sqrt{3}}\{|LL\rangle + |RR\rangle + |LR\rangle\}$ (d) $\frac{1}{2}\{|LL\rangle + |RR\rangle + |LR\rangle + |RL\rangle\}$. The envelope of $|\text{concurrence}|^2$ has a time dependence similar to the Shannon (spatial) entropy.

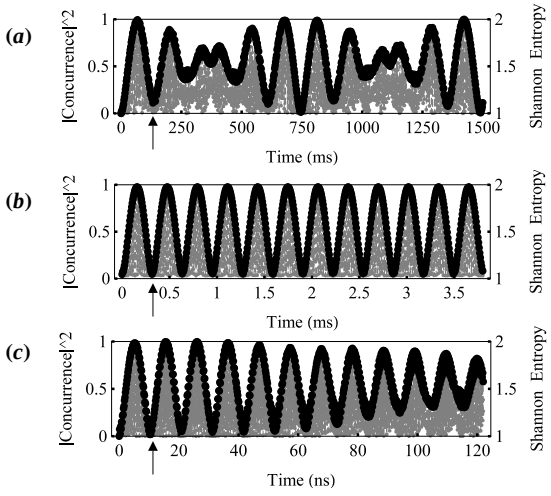

FIG. 4: Time evolution of Shannon entropy (black) and $|\text{concurrence}|^2$ (gray) for the initial state $\frac{1}{\sqrt{2}}\{|LL\rangle + |RR\rangle\}$ ($\frac{1}{\sqrt{2}}\{|\uparrow\uparrow\rangle + |\downarrow\downarrow\rangle\}$) for (a) Two ^6Li atoms in an optically created double well, (b) Two spins (two $^{25}Mg^+$ ions in different hyperfine ground states), (c) Two electrons in two separate DQDs. The envelope seen for each system is given by Eq. (7) and is a sum of cosines with frequencies $\omega_a = \frac{E_4 - E_3}{\hbar}$ and $\omega_b = \frac{E_2 - E_1}{\hbar}$, the values of ω_a and ω_b specific to each system. The Shannon entropy and the envelope of the $|\text{concurrence}|^2$ have a similar time dependence. The arrows indicate the time scales ($\frac{h}{2(E_4 - E_3)}$).